Journal of
Water & Climate Change

IWA PUBLISHING

Journal of Water and Climate Change Vol 13 No 4, 1830 doi: 10.2166/wcc.2022.440

Future precipitation changes in the Central Ethiopian Main Rift under CMIP5 GCMs

Wondimu T. Hailesilassie [a,*], Narendra K. Goel[b], Tenalem Ayenew[c] and Sirak Tekleab[d]

[a] College of Natural and Computational Sciences, African Canter of Excellence for Water Management, Addis Ababa University, Addis Ababa, Ethiopia
[b] Department of Hydrology, Indian Institute of Technology Roorkee, Roorkee 247667, India
[c] Schools of Earth Sciences, College of Natural and Computational Sciences, Addis Ababa University, Addis Ababa, Ethiopia
[d] Department of Water Resources and Irrigation Engineering, Hawassa University, Hawassa, Ethiopia
*Corresponding author. E-mail: wonde721@gmail.com

WTH, 0000-0002-3699-2799

ABSTRACT

The purpose of this study is to predict future changes in precipitation in the Central Ethiopian Main Rift, which is vulnerable to climate change. The Long Ashton Research Station Weather Generator (LARS-WG) model was applied to project precipitation based on five global climate models (GCMs) (EC-EARTH, MIROC-ESM, HadGEM2-ES, INM-CM4, and CCSM4) from Coupled Model Intercomparison Project phase 5 (CMIP5) under two representative concentration pathways (RCP4.5 and RCP8.5) in the periods of 2041–2060 compared to the baseline period of 1976–2005. The model's calibration and validation results showed that it could predict future precipitation. According to the analysis, the mean rainfall is expected to increase in January (up to 14.2%) and December (up to 27.8%) under the RCP 4.5 and RCP 8.5 scenarios, respectively. However, a drop is anticipated in June (up to 8.2%) and May (up to 7%) under the RCP 4.5 and RCP 8.5 scenarios, respectively. In both scenarios, summer precipitation (usually the rainy season) is predicted to fall, while winter precipitation (usually the dry season) is expected to climb. Furthermore, annual and spring precipitation forecasts are anticipated to decrease in most locations. The findings of this research will be utilized to guide future water resource management in the study region.

Key words: Central Ethiopian Main Rift, CMIP5, future precipitation, GCMs, LARS-WG

HIGHLIGHTS

- The multi-model ensemble (MME) mean of CMIP5 global climate model (GCM) outputs was used to address uncertainty associated with a single GCM.
- Precipitation is anticipated to decrease during the regularly wet season while increasing during the normally dry season in the years 2041–2060.
- The projected mean annual, seasonal, and monthly rainfall could be used to influence future water resource management in the Central Ethiopian Main Rift.

GRAPHICAL ABSTRACT

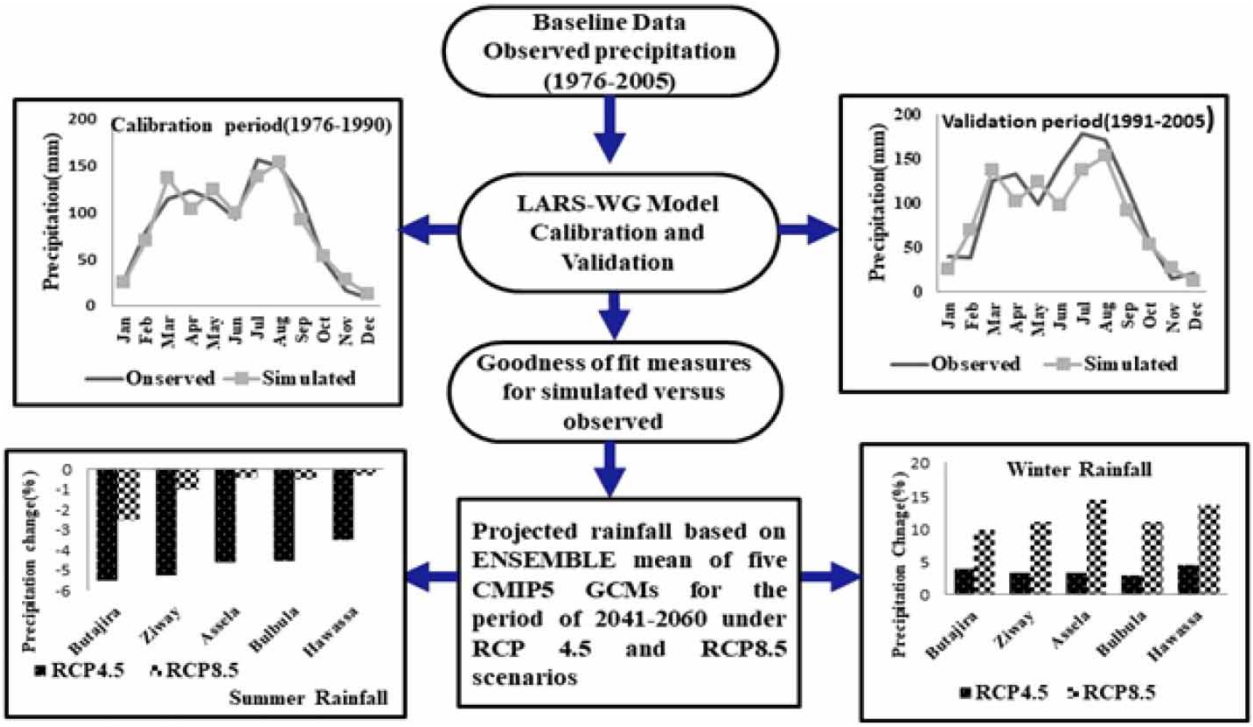

INTRODUCTION

The increase in the atmospheric concentrations of greenhouse gases, most notably carbon dioxide, has led to long-term climate change, which has been observed at global, regional, and ocean basin scales. Among them are changes in precipitation amounts and timings, arctic temperatures, and various types of extreme weather, such as heavy rain, droughts, and heatwaves (IPCC 2007). Africa, particularly East Africa, is extremely vulnerable to climate change, with more extreme events such as frequent droughts, floods, and heavy rains expected in the future (Gebrechorkos *et al.* 2019). A number of research studies on the future climate change scenario in the Central Ethiopian Main Rift (CEMR) have been conducted. For example, Zeray *et al.* (2009) used the statistical down scaling model (SDSM) to downscale precipitation in the Ziway Lake watershed of CEMR, from 2001 to 2099, based on HadCM3 (Hadley Centre Coupled Model, version 3) GCM (general circulation model) outputs under A2 and B2 SRES (Special Report on Emission Scenarios). They discovered that, based on the seasonal pattern, the spring season is more likely to have a lower total precipitation share than the other seasons. The winter season, on the other hand, may see a rise in overall share. Abraham *et al.* (2018) employed multi-model results from three Coupled Model Intercomparison Project phase 5 (CMIP5) GCMs (HadGEM2-ES, CSIROMK-3-6-0, and CCSM4 models) under representative concentration pathway (RCP) scenarios (RCP4.5 and RCP8.5) over the Lake Ziway Catchment in the CEMR. The results of the GCMs were retrieved from the KNMI climate explorer web page. Their findings indicated that precipitation will decrease in the future periods (the 2020s, 2050s, and the 2080s). Kassie *et al.* (2014) used four GCMs (HadCM3, CSIRO2, CGCM2, and PCM) and two emission scenarios, SRES (A2 and B1) to investigate future rainfall projections in the CEMR for the 2080s relative to the 1971–90 baseline periods. The climate change scenario data for these GCM-SRES combinations were extracted from the Tyndall Centre for Climate Change's TYN CY 3.0 data set. According to their findings, rainfall will increase outside of the growing season (November–December), but decrease during the growing season.

The outputs of GCMs are coarse; they must be downscaled to very fine resolution, or even to a local or station scale. In general, there are two types of downscaling methods widely used to transform coarse-scale information to a finer scale: dynamic and statistical downscaling (Ekström *et al.* 2015). As a result, Gebrechorkos *et al.* (2019) recommended adopting statistical downscaling models rather than dynamic downscaling methods for East Africa. This could be due to the fact that statistical models are quick, easy, and effective, requiring fewer computational resources and costs. Semenov &

Barrow (1997) and Semenov (2008) used the Long Ashton Research Station Weather Generator (LARS-WG), which is one of the most well-known statistical downscaling tools for assessing the impact of climate change. It is a computationally inexpensive downscaling tool for generating local-scale climate scenarios from global or regional climate models. It simulates time series of daily weather at a single site.

In recent years, many studies have been conducted to assess the future precipitation changes using the LARS-WG model. For instance, Khoi *et al.* (2021) used the LARS-WG tool to predict future climate in the Be River Basin in Southern Vietnam using an ensemble of five CMIP5 GCMs (Can-ESM2, CNRM-CM5, HadGEM2-AO, IPSL-CM5A-LR, and MPI-ESM-MR) under two RCP scenarios (RCP4.5 and RCP8.5). They discovered that annual precipitation will decrease by 4.0% in the 2030s and rise by 1.6 and 6.4% in the 2050s and 2070s for the RCP4.5. According to RCP8.5, annual precipitation will decrease by 4.5 and 0.6% in the 2030s and 2050s, respectively, then increase by 5.1% in the 2070s. Chisanga *et al.* (2017) tested the LARS-WG model to see if it could generate synthetic weather data for 2020 and 2055 based on HadCM3 and BCCR-BCM2 GCM predictions under SRB1 and SRA1B scenarios at Mount Makulu, Zambia. They found that precipitation amounts would increase in 2020 and 2055, based on the ensemble mean of HadCM3 and BCM2 GCMs.

Prior research in Ethiopia employed the previous version 5.5 LARS-WG model to estimate future climate change, which was based on Special Emissions Scenarios SRES (A1B and B1) from the Coupled Model Intercomparison Projects phase 3 (CMIP 3) GCMs and the IPCC's Fourth Assessment Report (AR4). For instance, Fenta & Disse (2018) used the LARS-WG 5.5 model to see if it could capture extreme events and daily precipitation distributions across the whole data range in Ethiopia's upper Blue Nile Basin. Furthermore, Disasa *et al.* (2019) applied the LARS-WG 5.5 model at the Hawassa site in Ethiopia's Rift Valley Lakes Basin and discovered that for all three time periods (2020s, 2055s, and 2090s), rainfall decreases in summer and increases in winter.

As a result, the current research used the LARS-WG model's latest version 6.0, which includes climate forecasts from the IPCC Fifth Assessment Report's (AR5) CMIP5 ensembles. According to Taylor *et al.* (2012), CMIP5 comprises more extensive models and enhanced experiments than CMIP3. Furthermore, higher spatial resolution models with a larger number of output fields are used in CMIP5.

Changes in precipitation patterns raise concerns about water resource management because extreme events such as droughts and floods are likely to become more frequent and severe in the future (Brekke *et al.* 2009). Hence, the LARS-WG model performed well in reflecting the statistical properties of observed climatic variables, including extreme events (Qian *et al.* 2008; Semenov 2008; Fenta & Disse 2018), which encouraged its adoption in the present study.

The prediction of changes in critical climate variables like precipitation is extremely important in order to make informed decisions about the management of the available water resources (Jayanta *et al.* 2015). The analysis of precipitation changes for the future is of great importance since the CEMR research region is mainly characterized by rain-fed agricultural activities. The purpose of this study is to project future precipitation change in the CMER by using the LARS-WG 6.0 model based on the ensemble mean of five CMIP5 GCMs (EC-EARTH, MIROC-ESM, HadGEM2-ES, INM-CM4, and CCSM4) under RCP4.5 and RCP8.5 scenarios for the period of 2041–2060. The study's findings will be used to guide future water resource management and planning in the CEMR region.

MATERIALS AND METHODS

Study area descriptions

This study focused on the CEMR, which consists of five lakes (Ziway, Abijata, Langano, Shalla, and Hawassa) and their watersheds with the Feeder Rivers, as shown in Figure 1. The CEMR is located at 38.22 and 39.31° E longitudes, and 6.75 and 8.47° N latitudes, with a total geographical area of about 15,880 km^2 (MoWR 2008). The topographic features of the CEMR were analyzed using the Shuttle Radar Topography Mission Digital Elevation Model (SRTM DEM) with a 30 m resolution (obtained from https://www.usgs.gov/). The maximum and minimum heights, based on DEM data, are 4,188 and 1,546 m (above mean sea level), respectively. The highlands are the sources of rivers and their tributaries that pour into the lakes, as shown in this diagram.

Meteorological data

The National Meteorological Agency (NMA) of Ethiopia provided daily time series of meteorological data (rainfall) for the period 1976–2005 (30 years) for this study. These data were utilized as a baseline for future climate data simulation

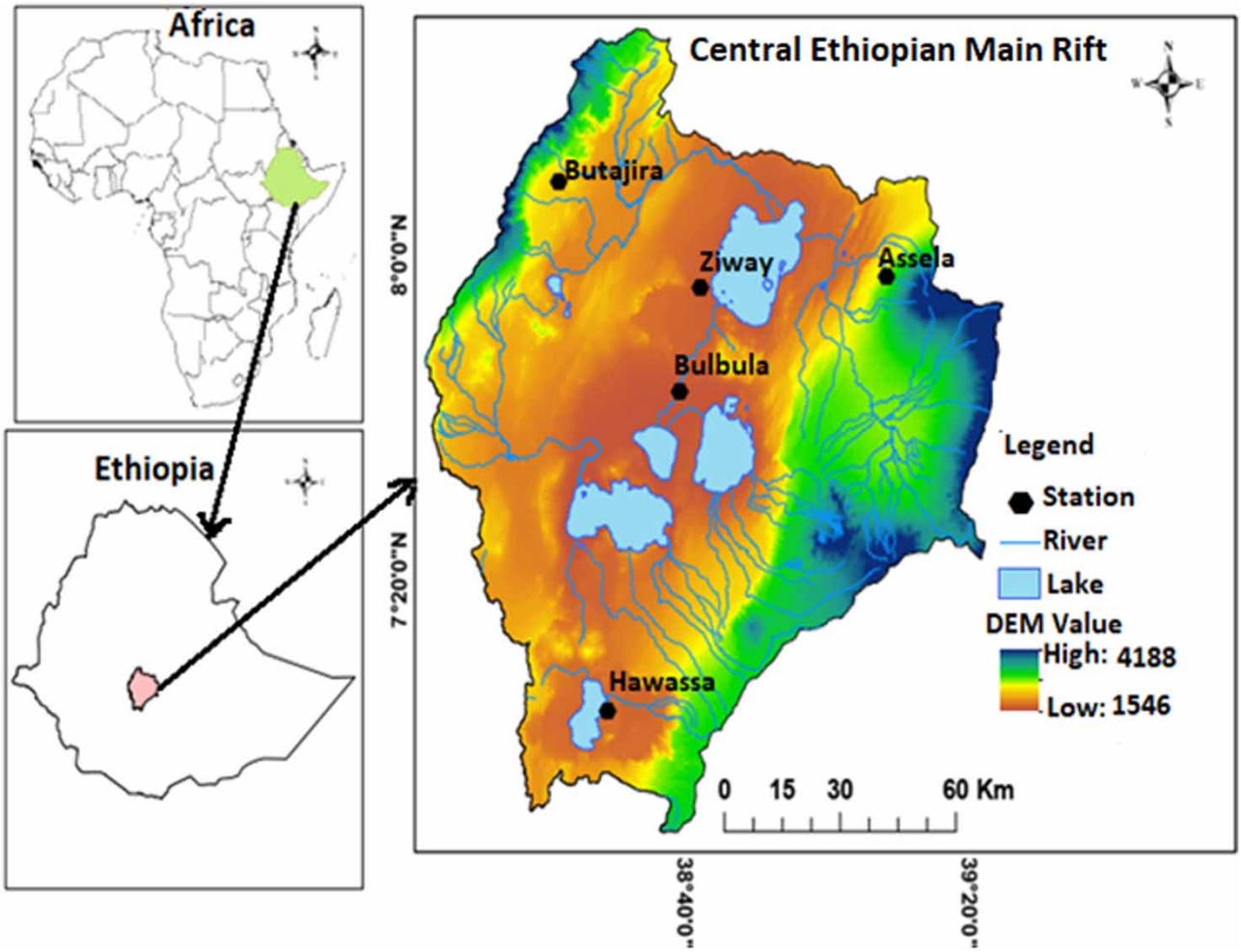

Figure 1 | Location map showing the CEMR with rivers, five lakes, and five meteorological stations online version of this paper to see this figure in colour: http://dx.doi.org/10.2166/wcc.2022.440.

(precipitation). Due to the limited data availability, five stations were used in this study, which are located in the northwest (e.g. Butajira), in the northeast (e.g. Assela), in the central (e.g. Ziway and Bulbula), and in the southern part of the basin (e.g. Hawassa). Figure 1 depicts the distribution of meteorological stations.

The climate of the study region is divided into three seasons: (i) the main rainy season in the summer (July–September), locally known as Kiremt rains, which account for 50–70% of annual rainfall totals; (ii) the short rainy season in the spring (March–May), known locally as Belg, which accounts for 20–30% of the yearly amount; and (iii) the dry season in the winter (October–January/February), known locally as Bega, which may have sporadic rains, accounts for 10–20% of the annual total (Legesse *et al.* 2004). Table 1 shows that the study region receives the annual mean rainfall between 717.68 and 1,089.27 mm, the summer mean rainfall between 407.74 and 617.89 mm, the spring mean rainfall between 205.68 and 353.14 mm, and the winter mean rainfall between 71.14 and 166.82 mm, regarding the time-series data from 1976 to 2005 (the baseline period of this study).

General circulation models

In the present study, as shown in Table 2, the output from the five CMIP5 GCMs (EC-EARTH, MIROC-ESM, HadGEM2-ES, INM-CM4, and CCSM4) were utilized to generate the future scenarios of rainfall for the period 2041–2060 (2050s) under two RCP scenarios (RCP 4.5 and RCP 8.5). RCP4.5 is an intermediate stabilization scenario with an equivalent concentration of CO_2 varying from 580 to 720 ppm in 2100, while RCP8.5 is a high emission scenario representing an equivalent concentration of CO_2 above 1,000 ppm in 2100 (IPCC 2013).

Table 1 | Mean rainfall for various time scales (annual, spring, summer, and winter) for 1976–2005 (the baseline period)

Station	Latitude	Longitude	Altitude	Mean rainfall			
				Annual	Summer	Spring	Winter
Butajira	8.15	38.37	2,000	1,087.93	560.55	353.14	115.16
Ziway	7.933	38.7	1,640	753.12	435.17	209.53	71.14
Assela	7.956	39.14	2,413	1,089.27	617.89	322.48	108.98
Bulbula	7.72	38.65	1,606	717.68	407.4	205.68	78.06
Hawassa	7.065	38.48	1,694	964.45	444.95	303.81	166.82

Table 2 | Five CMIP5 GCMs used in this study

Institute (modeling center)	Model name	Atmospheric resolution
European Community Earth-System, consortium, Europe	EC-EARTH	1.125°×1.125°
Met Office Hadley Centre, UK	HadGEM2-ES	1.25°×1.88°
National Institute for Environmental Studies, The University of Tokyo, Japan	MIROC-ESM	2.8125°×2.8125°
Institute for Numerical Mathematics(INM), Russia	INM-CM4	1.5°×2°
Community Climate System Model(CCSM), National Centre for Atmospheric Research(NCAR), USA	CCSM4	0.9°×1.25°

The uncertainties originate from the selection of the emission scenarios, GCM outputs, downscaling techniques, and hydrological models (Hoan *et al.* 2018; Vesely *et al.* 2019). In this study, for assessing the future precipitation simulation, the multimodel ensemble (MME) mean approach with different climate scenarios was utilized, which could help to reduce the uncertainty associated with using a single climate emission scenario and GCM in climate predictions (Fenta & Disse 2018; Bekele *et al.* 2021; Khoi *et al.* 2021).

Description of LARS-WG stochastic weather generator

This study employed the latest version, 6.0 LARS-WG, to simulate future climate change for the period 2041–2060 (2050s), which integrates climate forecasts from the CMIP5 used in the IPCC Fifth Assessment Report (AR5) (Table 2). Version 6.0 of the LARS-WG is available for download at https://sites.google.com/view/lars-wg/. LARS-WG is a stochastic weather generator, which can be used for the simulation of weather data in the form of daily time series at a single site under both current and future climate conditions. LARS-WG uses observed daily weather data for a given site to compute a set of parameters for probability distributions of weather variables as well as correlation between them. These parameters are then used to generate synthetic weather time series of arbitrary length by randomly selecting values from the appropriate distributions. LARS-WG uses a semi-empirical distribution (SED) that is known as the cumulative probability distribution function (CDF) approximate probability distribution of daily weather data (Semenov & Barrow 1997; Semenov & Stratonovitch 2010).

Hence, for each climatic variable v, a value of climatic variable v_i corresponding to the probability p_i is computed using the following equation:

$$V_i = \min\{v{:}P(v_{\text{obs}} \le v) \ge p_i\} i = 0, \ \ldots, \ n \tag{1}$$

where $P(\,)$ is probability of the observed variable v_{obs}.

Because the probability of very low daily precipitation (<1 mm) is typically relatively high and such low precipitation has very little effect on the output of a process-based impact model, only two values are used, v_1=0.5 mm and v_2=1 mm to approximate precipitation within the interval [0, 1] with the corresponding probabilities calculated as: $p_i = p(v_{\text{obs}} \le v_i), \ i = 1, \ 2$. To account for extremely high long dry and wet series, two values close to 1 are used in SEDs for wet and dry series, p_{n-1}=0.99 and v_{n-2}=0.98 (Semenov 2007; Semenov & Stratonovitch 2010).

Summary of the modeling process with LARS-WG

The modeling method for generating synthetic weather data in LARS-WG can be divided into three steps: model calibration, model validation, and generation of synthetic weather data. The following are brief descriptions of these steps: (i) model calibration is done to use the function 'SITE ANALYSIS' in LARS-WG, which analyses observed weather data (e.g. precipitation) to determine their statistical characteristics; (ii) model validation helps analyze and compare the statistical characteristics of the observed and synthetic weather data to assess the ability of LARS-WG to simulate the parameters in the chosen sites in order to determine whether or not it is suitable for use in the study; and (iii) the parameter files derived from the observed weather data during the model calibration process can also be used to generate synthetic weather data corresponding to a particular climate change scenario simulated by GCMs (Racsko *et al.* 1991; Semenov & Barrow 2002).

LARS-WG model performance evaluation

In order to test the performance of the LARS-WG model and ensure its ability to predict future precipitation in this study, the coefficient of determination (R^2) and the root-mean-square error (RMSE) were employed to compare observed and simulated rainfall data (Hassan *et al.* 2014; Bayatvarkeshi *et al.* 2020; Khoi *et al.* 2021). R^2 is a dimensionless measure whose optimal value is one, as shown in Equation (2). Moreover, in Equation (3), the RMSE denotes the model error rate, with the optimal value being zero.

$$R^2 = \frac{\left(\sum_{i=1}^{n}(x-\bar{x})\right)(y-\bar{y}))^2}{\sum_{i=1}^{n}(x-\bar{x})^2(y-\bar{y})^2} \tag{2}$$

$$\text{RMSE} = \sqrt{\frac{(x-y)^2}{n}} \tag{3}$$

where x and y are the observed and simulated values, respectively; $\bar{x}$ and $\bar{y}$ are the average of X and Y; and n is the total number of data.

The mean rainfall is compared graphically to the observed data to boost confidence in the analyses' performance. The model's patterns and variations can be identified using these graphical comparisons. As a result, the LARS-WG was calibrated and validated in this work utilizing rainfall from five rain gauges from 1976 to 2005 (Figure 1). The calibration and validation processes took place from 1976 to 1990 and 1991 to 2005, respectively.

The LARS-WG model was used to generate future rainfall scenarios based on five GCM outputs acquired from CMIP5 GCMs (Table 2) for the 2050s (2041–2060) under two emission scenarios: RCP4.5 and RCP8.5, after successful calibration and validation against historical data from 1976 to 2005. The LARS-WG model's future precipitation projections in the study area were compared to previous studies.

RESULTS AND DISCUSSION

Analysis of the LARS-WG calibration and validation results

The daily time series of precipitation data from 1976 to 2005, selected as the baseline year, was used in this study for the calibration and validation of the LARS-WG model. The calibration and validation processes took place from 1976 to 1990 and 1991 to 2005, respectively.

The performance statistics results of the downscaled monthly rainfalls simulated by LARS-WG during calibration and validation periods are shown in Table 3. The R^2 value between observed and simulated monthly precipitation is reasonable, ranging from 0.92 to 0.99 in the calibration period and 0.826 to 0.908 in the validation period. Furthermore, for the calibration and validation periods, the RMSE values ranged from 7.0 to 13.74 and 11.44 to 25.431 mm, respectively. Monthly mean values of observed and synthetic data for the calibrated and validated periods are also remarkably consistent across all rain gauges, as shown in Figure 2(a) and 2(b), with monthly simulated and observed precipitation differences ranging from 0.52 to 2.69 mm/month for the calibration and 0.99 to 8.86 mm/month for the validation.

Table 3 | Performance statistics of LARS-WG results against historical observed rainfall data during calibration and validation periods

	Calibration period (1976–1990)		Validation period (1991–2005)	
Meteorological station	R^2	**RMSE**	R^2	**RMSE**
Butajira	0.921	13.741	0.826	25.431
Ziway	0.971	7.358	0.941	11.44
Assela	0.973	10.574	0.894	22.446
Bulbula	0.987	7.002	0.908	12.114
Hawassa	0.957	8.125	0.865	14.365

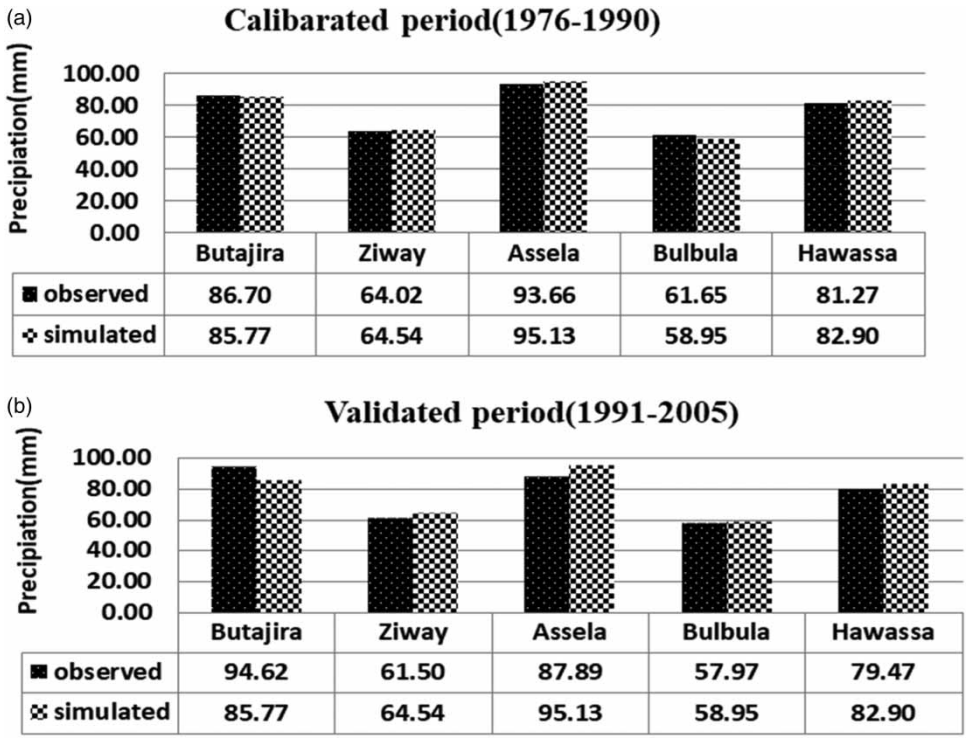

Figure 2 | Monthly mean observed and simulated rainfall for calibration period (a) and validation period (b).

Based on these findings, LARS-WG performance in reproducing historical climate is deemed satisfactory, and it can be used to forecast the future precipitation with reasonable accuracy.

Analysis of future precipitation changes

Analysis of the future monthly mean precipitations changes

The percentage changes in the monthly mean precipitation values for the future periods compared to the baseline period are shown in Table 4 and in Figure 3(a) and 3(b). According to Table 4, we can see that in most stations, the forecast of the monthly mean precipitation changes by CCSM4 and HadGEM2-ES is expected to increase. This result agrees with Jury (2014). Also in Table 4, it can be seen that CCSM4 predicts the biggest rise (up to 18.83%) in the monthly mean precipitation for Hawassa, while INM-CM4 predicts the highest drop (up to 4.75%) for Assela. The monthly mean rainfall is expected to decrease and increase in most of the stations, according to the GCM outputs of EC-EARTH, MICRO-ESM, and INM-CM4.

As a result, there are inconsistencies in the GCM outputs for each site/area. These findings suggest that utilizing a single GCM to forecast future precipitation is fraught with uncertainty; hence, an attempt was made in this work to calculate the

Table 4 | Percentage change in monthly mean precipitation in the future period (2040–2061) based on each of the five CMIP5 GCMs under RCP 4.5 and RCP 8.5 scenarios compared to the baseline period (1976–2005)

Station	Scenario	EC-EARTH	MIROC-ESM	CCSM 4	HadGEM2-ES	INM-CM4
Butajira	RCP4.5	−3.67	−0.33	3.92	−0.50	−3.42
	RCP8.5	10.08	0.17	7.42	−1.58	−3.42
Assela	RCP4.5	0.83	−2.75	8.25	2.00	−4.75
	RCP8.5	12.92	−0.17	12.50	3.08	7.00
Ziway	RCP4.5	−1.33	−1.42	6.58	0.75	−3.75
	RCP8.5	10.50	0.08	10.67	0.50	7.83
Bulbula	RCP4.5	−1.33	−0.92	9.58	1.00	−3.67
	RCP8.5	9.33	−0.50	12.42	0.42	8.00
Hawassa	RCP4.5	−1.92	−0.25	18.83	2.17	−2.67
	RCP8.5	5.67	−1.42	18.25	3.50	9.17

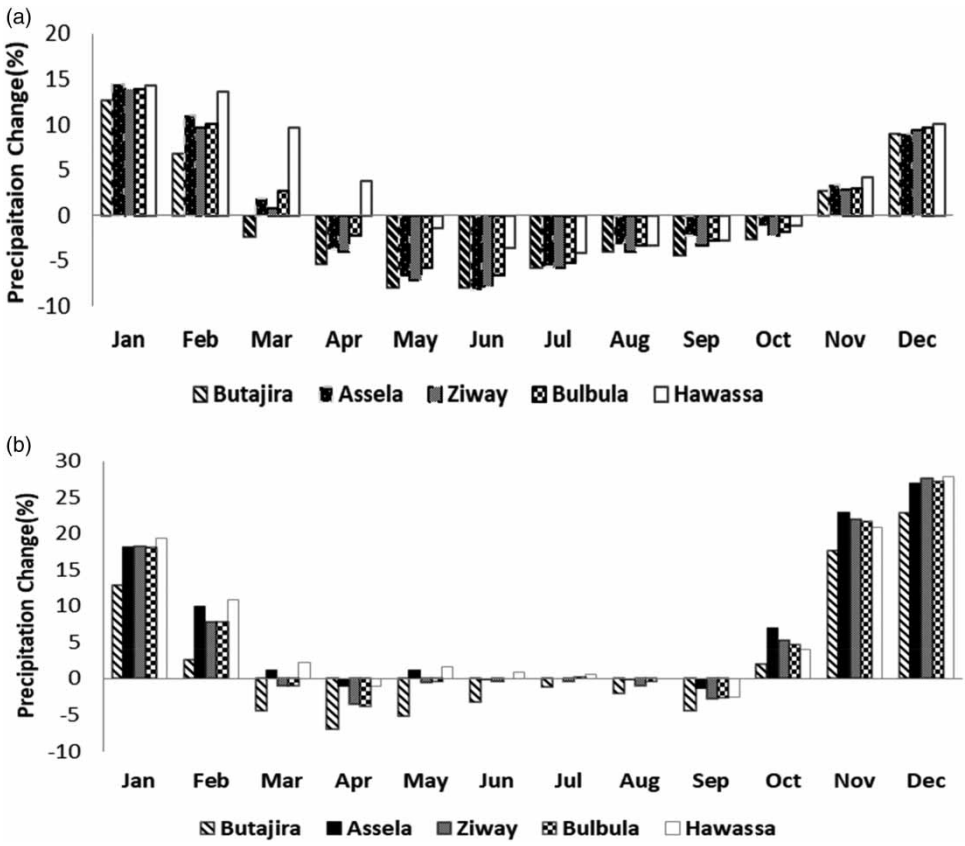

Figure 3 | Percentage changes in the average monthly rainfall from the ensemble mean of five GCMs under (a) the RCP 4.5 scenario and (b) the RCP 8.5 scenario.

mean value of the precipitation forecasts from five GCMs, which are mentioned in the subsequent sections (the annual and seasonal mean precipitation forecasts) in order to further illustrate the future change in the period from 2041–2060.

According to Figure 3(a) and 3(b), the percentage changes in the monthly average precipitation for all stations for both scenarios (RCP 4.5 and RCP 8.5) in the entire catchment area for the future periods followed almost a similar pattern. In

those figures, we can also see that all sites would expect the highest increased monthly rainfall (floods) in January (up to 14.2%) and December (up to 27.8%) in the RCP 4.5 and RCP8.5 scenarios, respectively. Meanwhile, the highest decline (droughts) is predicted in June (up to 8.2%) and in May (up to 7%) under the RCP 4.5 and RCP 8.5 scenarios, respectively. As a result of these data, it can be concluded that rainfall is expected to increase continuously during the dry season (October–January), while rainfall is expected to decrease or stay close to the baseline monthly rainfall during the wet months (March–September) of the study area under both the scenarios.

Analysis of future changes in annual and seasonal mean precipitation

Figures 4(a) and 4(b) and 5(a) and 5(b) depict the ensemble averages of precipitation forecasts from the five CMIP5 GCMs (Table 2), calculated to further illustrate the future changes in the annual and seasonal timescales over the period (2041–2060) compared to the baseline period (1976–2005) under the RCP 4.5 and RCP 8.5 scenarios. Figure 4(a) and 4(b) shows that rainfall in the basin is predicted to drop by up to 3.8 and 5.5% in the annual and spring seasons, respectively, under both scenarios for all stations except Hawassa (under both scenarios) and Assela (close to the baseline rainfall under the RCP8.5 scenario). Figure 5(a) and 5(b) shows that summer and winter rainfall patterns are forecast to be opposite in all sites; hence, rainfall is expected to decrease in summer (extended rainy season), while rainfall is expected to increase in winter (dry season) under both the scenarios. This finding is in line with previous studies in the research area (Kassie *et al.* 2014; Abraham *et al.* 2018; Disasa *et al.* 2019). Figures 4(a) and 4(b) and 5(a), comparing all stations, Butajira sites (north western part of the basin), exhibit relatively the highest decrease in annual, spring, and summer rainfall under both the scenarios. Moreover, Figure 5(a) and 5(b) depicts under the RCP8.5 scenario, unseasonal rainfall will be expected during the dry season, but the RCP 4.5 scenario predicts a noticeable reduction in summer rainfall for all sites. According to those figures, we can infer that extreme precipitation events, such as droughts in the summer (normally the rainy season) and flooding in the winter (normally the dry season), are predicted under the RCP4.5 and RCP8.5 scenarios respectively.

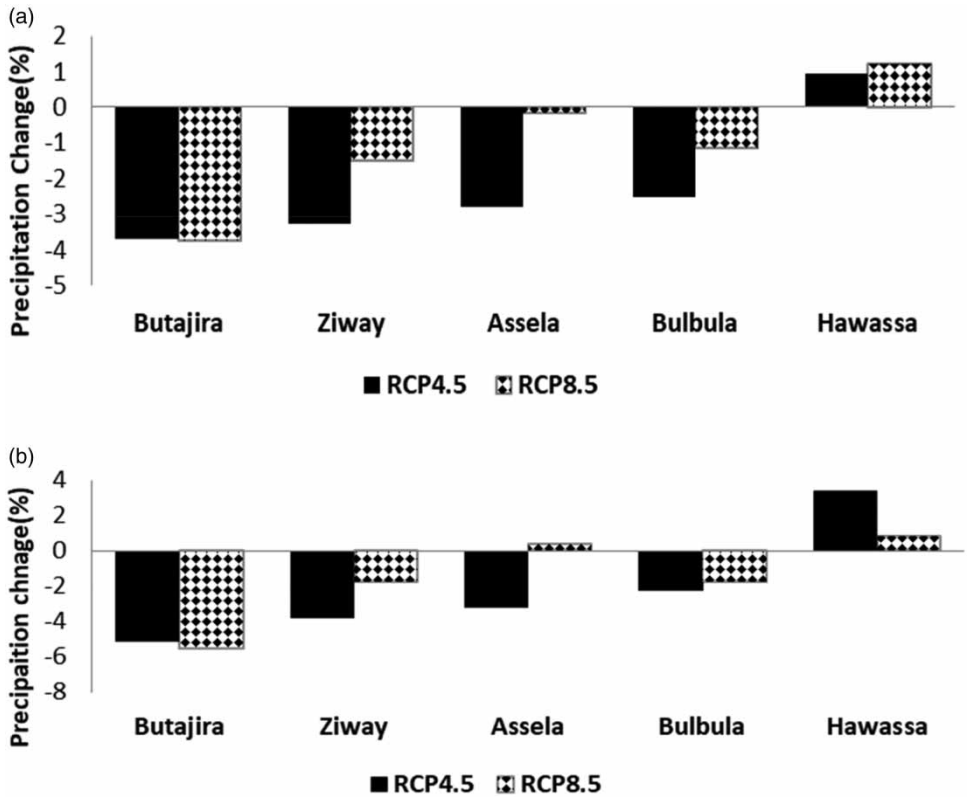

Figure 4 | Percentage changes in the mean precipitation for five sites (a) in annual rainfall and (b) in spring rainfall.

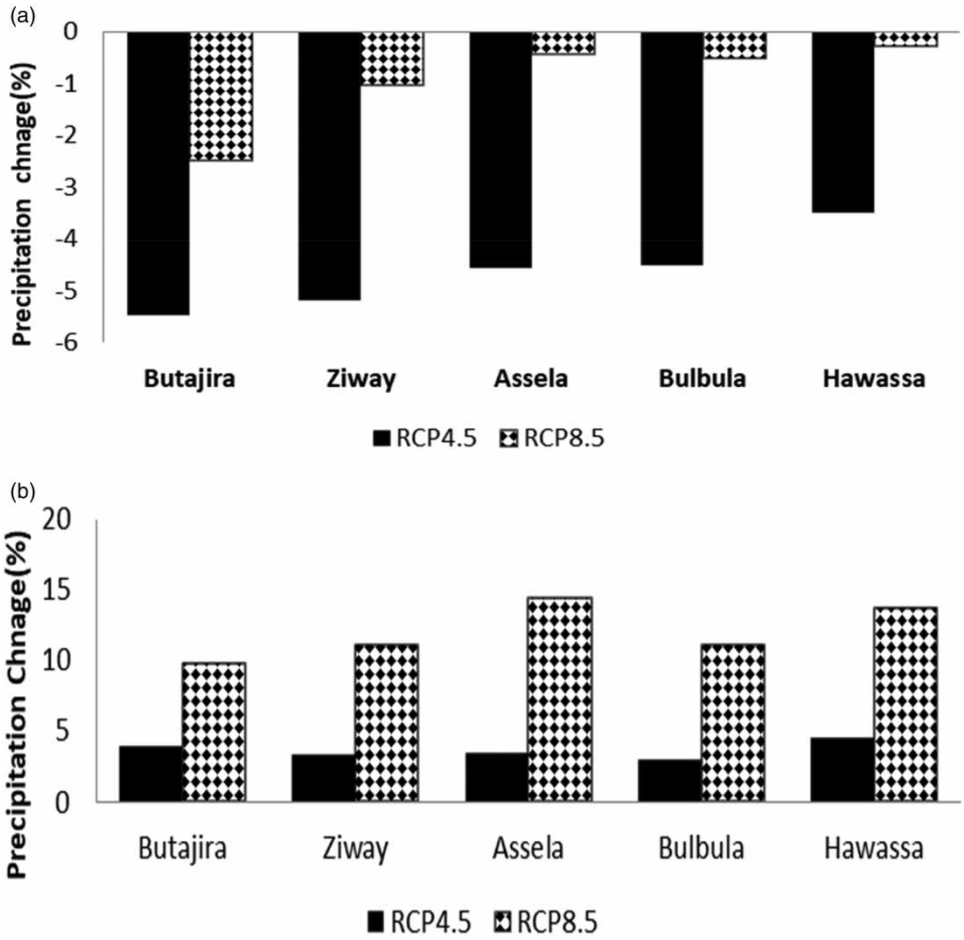

Figure 5 | Percentage changes in the mean precipitation for five sites in (a) summer rainfall and (b) winter rainfall.

CONCLUSIONS

In the present study, we used the LARS-WG stochastic weather generator to analyze future precipitation changes across the CEMR in the period of 2041–2060. The observed rainfall data for the period of 1976 to 2005 were selected as the baseline year for comparison with future scenarios. The calibration and validation processes took place from 1976 to 1990 and 1991 to 2005, respectively.

The performance evaluation of the LARS-WG model revealed that the model illustrates a satisfactory agreement between the observed and simulated rainfall. The results revealed the increased mean rainfall in January (up to 14.2%) and December (up to 27.8%) under the RCP 4.5 and RCP8.5 scenarios, respectively. However, a drop is expected in June (up to 8.2%) and May (up to 7%) under the RCP 4.5 and RCP 8.5 scenarios, respectively. Summer precipitation is expected to decrease, while winter precipitation is expected to increase at all locations in both scenarios. A noticeable reduction in summer rainfall is predicted under the RCP 4.5 scenario for all sites. The RCP 8.5 scenario predicts unseasonal rainfall during the dry season. Predicting rainfall below normal can improve the use of water abstraction techniques to alleviate the problem of water scarcity in the study region characterized by rain-fed agricultural activities. Predicting above average and unusual rainfall throughout the winter season is critical to reducing the risk of flooding and crop damage during harvest.

In the present work, in order to address the uncertainty associated with a single emission scenario and GCM, we used the ensemble mean of five CMIP5 GCM outputs (EC-EARTH, MIROC-ESM, HadGEM2-ES, INM-CM4, and CCSM4) under the RCP4.5 and RCP8.5 scenarios. Additional downscaling techniques (apart from LARS-WG) and hydrological modeling tools, on the other hand, are not considered in our analysis. More GCMs, emission scenarios, downscaling techniques, and

hydrological modeling tools for climate change impacts on water resources are all needed to improve these results. Further research will be required to take into account the limitations of this study in addressing all uncertainties. The findings of this study can be used to establish future sustainable water resource management and planning for a variety of fields, including water resources and agriculture.

ACKNOWLEDGEMENTS

The authors would like to thank the National Meteorological Agency of Ethiopia for providing meteorological data for this study. We are also grateful to the editors and two anonymous reviewers for their insightful comments and suggestions, which have improved the quality of this paper.

CONFLICT OF INTEREST

The authors declare no conflict of interest.

DATA AVAILABILITY STATEMENT

All relevant data are included in the paper or its Supplementary Information.

REFERENCES

Abraham, T., Woldemicheala, A., Muluneha, A. & Abateb, B. 2018 Hydrological responses of climate change on Lake Ziway Catchment, Central Rift Valley of Ethiopia. *Journal of Earth Science and Climatic Change* **9**, 474.

Bayatvarkeshi, M., Zhang, B., Fasihi, R., Adnan, R. M., Kis, O. & Yuan, X. 2020 Investigation into the effects of climate change on reference evapotranspiration using the HadCM3 and LARS-WG. *Water* **12** (3), 666.

Bekele, W. T., Haile, A. T. & Rientj, T. 2021 Impact of climate change on the streamflow of the Arjo-Didessa catchment under RCP scenarios. *Journal of Water and Climate Change* **12** (6), 2325–2337.

Brekke, L. D., Kiang, J. E., Olsen, J. R., Pulwarty, R. S., Raff, D. A., Turnipseed, D. P., Webb, R. S. & White, K. D. 2009 Climate change and water resources management – a federal perspective. *U.S. Geological Survey Circular* **1331**, 65.

Chisanga, C. B., Phiri, E. & Chinene, V. R. N. 2017 Statistical downscaling of precipitation and temperature using Long Ashton Research Station weather generator in Zambia: a case of Mount Makulu Agriculture Research Station. *American Journal of Climate Change* **6**, 487–512.

Disasa, K. N., Tura, F. S. & Fereda, M. E. 2019 Climate change downscaling using stochastic weather generator model in Rift Valley Basins of Ethiopia. *American Journal of Climate Change* **8**, 561–590.

Ekström, M., Grose, M. R. & Whetton, P. H. 2015 An appraisal of downscaling methods used in climate change research. *WIREs Climate Change* **6**, 301–319.

Fenta, D. K. & Disse, M. 2018 Analysing the future climate change of Upper Blue Nile River basin using statistical downscaling techniques. *Hydrology and Earth System Sciences* **22**, 2391–2408.

Gebrechorkos, S. H., Hülsmann, S. & Bernhofer, C. 2019 Statistically downscaled climate dataset for East Africa. *Science Data* **6**, 31.

Hassan, Z., Shamsudin, S. & Harun, S. 2014 Application of SDSM and LARS-WG for simulating and downscaling of rainfall and temperature. *Theoretical and Applied Climatology* **116**, 243–257.

Hoan, N. X., Nguyen, X., Khoi, D. N. & Pham, N. T. 2018 Uncertainty assessment of stream flow protection under the impact of climate change in the Lower Mekong Basin: a case study of the Srepok River Basin, Vietnam. *Water and Environment Journal* **34**, 1–12.

IPCC 2007 Summary for Policymakers. In: *Climate Change 2007: The Physical Science Basis. Contribution of Working Group I to the Fourth Assessment Report of the Intergovernmental Panel on Climate Change* (S. Solomon, D. Qin, M. Manning, Z. Chen, M. Marquis, K. B. Averyt, M. Tignor & H. L. Miller, eds.). Cambridge University Press, Cambridge, UK and New York, NY, USA.

IPCC 2013 *Climate Change 2013: The Physical Science Basis. Contribution of Working Group I to the Fifth Assessment Report of the Intergovernmental Panel on Climate Change*. Cambridge University Press, Cambridge, UK and New York, NY, USA.

Jayanta, J., Chicholikar, J. & Rathore, L. 2015 Predicting future changes in temperature and precipitation in arid climate of Kutch, Gujarat: analyses based on LARS-WG model. *Current Science* **109**, 11.

Jury, M. R. 2014 Statistical evaluation of CMIP5 climate change model simulations for the Ethiopian highlands. *International Journal of Climatology* **35**, 37–44.

Kassie, B. T., Rötter, R. P., Hengsdijk, H., Asseng, S., Van Ittersum, M. K., Kahiluoto, H. & Van keulen, H. 2014 Climate variability and change in the Central Rift Valley of Ethiopia: challenges for rainfed crop production. *The Journal of Agricultural Science* **152** (1), 58–74.

Khoi, D. N., Sam, T. T., Loi, P. T., Hung, B. V. & Nguyen, V. 2021 Impact of climate change on hydro-meteorological drought over the Be River Basin, Vietnam. *Journal of Water and Climate Change* **12** (7), 3159–3169.

Legesse, D., Coulomb, C. & Gasse, F. 2004 Analysis of the hydrological response of a tropical terminal lake, Lake Abiyata (Main Ethiopian Rift Valley) to changes in climate and human activities. *Journal of Hydrological Processes* **18**, 487–504.

MoWR (The Federal Democratic Republic of Ethiopia Ministry of Water Resources) 2008 *Rift Valley Lakes Basin Integrated Resources Development Master Plan Study Project*. Halcrow Group Limited and Generation Integrated Rural Development (GIRD) Consultants, Addis Ababa, Ethiopia.

Qian, B., Gameda, S. & Hayhoe, H. 2008 Performance of stochastic weather generators LARS-WG and AAFC-WG for reproducing daily extremes of diverse Canadian climates. *Climate Research* **37**, 17–33.

Racsko, P., Szeidl, L. & Semenov, M. A. 1991 A serial approach to local stochastic weather models. *Ecological Modelling* **57**, 27–41.

Semenov, M. A. 2007 Development of high-resolution UKCIP02-based climate change scenarios in the UK. *Agricultural and Forest Meteorology* **144**, 127–138.

Semenov, M. A. 2008 Simulation of extreme weather events by a stochastic weather generator. *Climate Research* **35** (3), 203–212.

Semenov, M. A. & Barrow, E. M. 1997 Use of a stochastic weather generator in the development of climate change scenarios. *Climatic Change* **35** (4), 397–414.

Semenov, M. A. & Barrow, E. M. 2002 LARS-WG. A Stochastic Weather Generator for Use in Climate Impact Studies. Version 3.0. User Manual. Available from: http://resources.rothamsted.ac.uk/sites/default/files/groups/mas-models/download/LARS-WG-Manual.pdf (accessed 4 Novemeber 2021).

Semenov, M. A. & Stratonovitch, P. 2010 Use of multi-model ensembles from global climate models for assessment of climate change impacts. *Climate Research* **41**, 1–14.

Taylor, K. E., Stouffer, R. J. & Meehl, G. A. 2012 An overview of CMIP5 and the experiment design. *Bulletin of American Meteorological Society* **93** (4), 485–498.

Vesely, F. M., Paleari, L., Movedi, E., Bellocchi, G. & Confalonieri, R. 2019 Quantifying uncertainty due to stochastic weather generators in climate change impact studies. *Scientific Reports* **9**, 9258.

Zeray, L. A., Roehrig, J. & Alamirew, D. C. 2009 Climate Change Impact on Lake Ziway Watershed Water Availability, Ethiopia. In: *CICD Series Vol.1: LARS 2007 Proceedings. May 7–11, 2007, Arba Minch, Ethiopia*. Available from: https://www.uni-siegen.de/zew/publikationen/cicd_series/cicd_vol.1_lars_2007-08.02.10.pdf (accessed 5 October 2020).

First received 10 November 2021; accepted in revised form 20 February 2022. Available online 3 March 2022